confirmed by the flight tests reported in Reference 4.3 and in other data from isolated sources.

DRAG BREAKDOWN AND EQUIVALENT FLAT-PLATE AREA

The parasite drag of an airplane can be estimated by estimating the drag of each component and then totaling the component drag while accounting for some interference drag. If C_{D_i} and S_i are the drag coefficient and reference area, respectively, for the ith component, then the total drag will be

$$\begin{aligned} D &= \tfrac{1}{2}\rho V^2 C_{D_1} S_1 + \tfrac{1}{2}\rho V^2 C_{D_2} S_2 + \cdots + \tfrac{1}{2}\rho V^2 C_{D_i} S_i + \cdots \\ &= \tfrac{1}{2}\rho V^2 (C_{D_1} S_1 + C_{D_2} S_2 + \cdots + C_{D_i} S_i + \cdots) \end{aligned} \tag{4.34}$$

Obviously, the drag coefficients of the components cannot be added since the reference areas are different. However, from Equation 4.34, the products $C_{D_i}S_i$ can be added. Such a product is referred to as the *equivalent flat-plate area*, f. One will also hear it referred to as the "parasite area" or simply, the "flat-plate area." The connotation "flat plate" is misleading, since it is not the area of a flat plate with the same drag. Instead, it is the reference area of a fictitious shape having a C_D of 1.0, which has the same drag as the shape in question. f is therefore simply D/q. It is a convenient way of handling the drag, since the f's of the drag components can be added to give the total f of an airplane.

$$\frac{D}{q} = C_{D_1} S_1 + C_{D_2} S_2 + \cdots$$

or

$$\begin{aligned} f &= \sum_{i=1}^{n} C_{D_i} S_i \\ &= \sum_{i=1}^{n} f_i \end{aligned} \tag{4.35}$$

This notation indicates that the flat-plate areas are to be summed for the ith component, from $i = 1$ to n where n is the total number of components.

DRAG COUNTS

As a measure of an airplane's drag, in practice one will frequently hear the term "drag count" used. Usually, it is used in an incremental or decremental sense, such as "fairing the landing gear reduced the drag by 20 counts." One drag count is defined simply as a change in the total airplane C_D, based on the wing planform area of 0.0001. Hence a reduction in drag of 20 counts could mean a reduction in the C_D from, say, 0.0065 down to 0.0045.

AVERAGE SKIN FRICTION COEFFICIENTS

In examples to follow, one will see that several uncertainties arise in attempting to estimate the absolute parasite drag coefficient (as opposed to incremental effects) of an airplane. These generally involve questions of interference drag and surface irregularities. In view of these difficulties, it is sometimes better to estimate the total drag of a new airplane on the basis of the known drag of existing airplanes having a similar appearance, that is, the same degree of streamlining and surface finish.

The most rational basis for such a comparison is the total wetted area and not the wing area, since C_f depends only on the degree of streamlining and surface finish, whereas C_D depends on the size of the wing in relation to the rest of the airplane. In terms of an average C_F, the parasite drag at zero C_L for the total airplane can be written as

$$D = qC_F S_w \tag{4.36}$$

where S_w is the total wetted area of the airplane. Since

$$f = \frac{D}{q}$$

it follows that the ratio of the equivalent flat-plate area to the wetted area is

$$\frac{f}{S_w} = C_F \tag{4.37}$$

In order to provide a basis for estimating C_F, Table 4.2 presents a tabulation of this quantity for 23 different airplanes having widely varying configurations. These range all the way from Piper's popular light plane, the Cherokee, to Lockheed's jumbo jet, the C-5A.

The data in this table were obtained from several sources and include results obtained by students taking a course in techniques of flight testing. Thus, the absolute value of C_F for a given airplane may be in error by a few percent. For purposes of preliminary design, the C_F ranges given in Table 4.3 are suggested for various types of airplanes. Where a particular airplane falls in the range of C_F values for its type will depend on the attention given to surface finish, sealing (around cabin doors, wheel wells, etc.), external protuberances, and other drag-producing items.

Additional drag data on a number of airplanes, including supersonic airplanes, are presented in Appendix A.3 as a function of Mach number and altitude.

Finally, with regard to average C_F values, Figure 4.26 (taken from Ref. 4.11) is presented. Although only a few individual points are identified on this figure, its results agree generally with Table 4.2. This figure graphically depicts the dramatic improvement in aerodynamic cleanliness of airplanes that has been accomplished since the first flight of the Wright Brothers.

Table 4.2 Typical Overall Skin Friction Coefficients for a Number of Airplanes Built from Approximately 1940 to 1976. Data Taken from Several Sources

C_F	Airplane Designation	Description
0.0100	Cessna 150	Single prop, high wing, fixed gear
0.0095	PA-28	Single prop, low wing, fixed gear
0.0070	B-17	Four props, World War II bomber
0.0067	PA-28R	Single prop, low wing, retractable gear
0.0066	C-47	Twin props, low wing, retractable gear
0.0060	P-40	Single prop, World War II fighter
0.0060	F-4C	Jet fighter, engines internal
0.0059	B-29	Four props, World War II bomber
0.0054	P-38	Twin props, twin-tail booms, World War II fighter
0.0050	Cessna 310	Twin props, low wing, retractable gear
0.0049	Beech V35	Single prop, low wing, retractable gear
0.0046	C-46	Twin props, low wing, retractable gear
0.0046	C-54	Four props, low wing, retractable gear
0.0042	Learjet 25	Twin jets, pod-mounted on fuselage, tip tanks
0.0044	CV 880	Four jets, pod-mounted under wing
0.0041	NT-33A	Training version of P-80 (see below)
0.0038	P-51F	Single prop, World War II fighter
0.0038	C-5A	Four jets, pod-mounted under wing, jumbo jet
0.0037	Jetstar	Four jets, pod-mounted on fuselage
0.0036	747	Four jets, pod-mounted under wing, jumbo jet
0.0033	P-80	Jet fighter, engines internal, tip tanks, low-wing
0.0032	F-104	Jet fighter, engines internal, midwing
0.0031	A-7A	Jet fighter, engines internal, high wing

Table 4.3 Typical Total Skin Friction Coefficient Values for Different Airplane Configurations

Airplane Configuration	C_F Range at Low Mach Numbers
Propeller driven, fixed gear	0.008–0.010
Propeller driven, retractable gear	0.0045–0.007
Jet propelled, engines pod-mounted	0.0035–0.0045
Jet propelled, engines internal	0.0030–0.0035

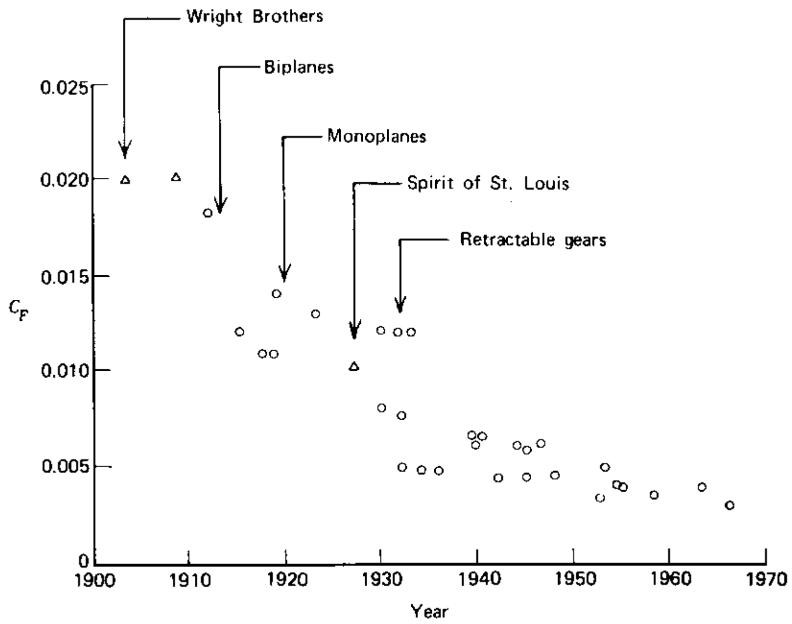

Figure 4.26 Historical survey of drag.

EXAMPLE ESTIMATES OF DRAG BREAKDOWN

The use of Equation 4.35 is illustrated in Table 4.4, where I have performed an estimate of the drag breakdown for the Cherokee (Figure 3.62). Armed with a tape measure, I made a visual inspection of the airplane, noting the dimensions of all drag-producing appendages. What you see here is a first estimate without any iteration. The total value for f of 0.36 m^2 (3.9 ft^2) is obviously too low and should be approximately 50% higher. This airplane has a total wetted area of approximately 58.06 m^2 (625 ft^2).

Undoubtedly, an aerodynamicist working continuously with this type of aircraft would be able to make a drag breakdown more accurate than the one shown in Table 4.4. Based on one's experience with his or her company's aircraft, the aerodynamicist can make more certain allowances for surface roughness, interferences and leakage. For example, in the case of the Cherokee's landing gear, the oleo struts have a bar linkage immediately behind them. The linkage, struts, wheel pants, and brake fittings produce a total drag for the entire landing gear that is probably significantly higher than the total f of 0.065 m^2 (0.7 ft^2) estimated for the wheels, wheel pants, and struts. The cylindrical oleo struts, in particular, being close to the wheel pants probably produce separation over the pants so that C_d for this item could be

Table 4.4 Drag Breakdown for Piper Cherokee 180

Item	Description	Reference Area	C_d	Basis for C_d	$F = C_dA$
Wing	See Figure 3.62	160 (plan)	0.0093	Figure 4.12 +50% for roughness	1.49
Fuselage	See Figure 3.62	15.2 (front)	0.058	Figure 4.13 $l/d_e = 5$	0.88
Horizontal tail	See Figure 3.62	25 (plan)	0.0084	Figure 4.12 +50% for roughness	0.21
Vertical tail	See Figure 3.62	11.5 (plan)	0.0084	Figure 4.12 +50% for roughness	0.10
Wheel struts	20 in. long 1.5 in. D half faired	0.63 (front)	0.3	Figure 4.6 supercritical	0.19
Wheel pants	12 in. high 7 in. wide streamlined	1.75 (front)	0.04	Figure 4.11	0.07
Wheels	6 in. below pants 5 in. wide	0.63 (front)	0.70	Figure 4.10 corrected to three-dimensional	0.44
Pitot-static tube	$\frac{1}{2}$ in. × 5 in. blunt/ rounded edge	0.02 (front)	1.0	Figure 4.7	0.02
Flap control horns	3 in. × $\frac{3}{4}$ in. blunt (6 total)	0.09 (front)	1.0	Figure 4.7*a*	0.09
Gas drain cocks	1 in. × $\frac{1}{2}$ in.blunt (2 total)	0.01 (front)	1.0	Figure 4.7	0.01
Rotating beacon	4 in. D × 5 in. semispherical	0.14 (front)	0.15	Figure 4.6	0.02
Tail tie-down	$3\frac{1}{2}$ in. × $\frac{3}{8}$ in. blunt	0.01 (front)	1.0	Figure 4.7	0.01
Wing tie-downs	1 in. × $\frac{3}{8}$ in. blunt (2)	0.01 (front)	1.0	Figure 4.7	0.01
Five whip antennas	$\frac{1}{4}$ in. D × 20 in. each	0.17 (front)	1.0	Figure 4.7 subcritical	0.17
Two pipes from engine step	3 in. D × 2 in. each	0.08 (front)	0.2	Figures 4.6 and 4.7*b*	0.02
	12 in. long, $\frac{3}{4}$ in. thick, 2 in. chord	0.06 (front)	0.06	Figure 4.11 +50% for roughness	0.04
OAT gage	3 in. × $\frac{3}{4}$ in. D blunt	0.02	1.0	Figure 4.7	0.02
Antenna fairing	3 in. deep × 6 in. width stream-lined	0.13	0.06	Figure 4.11 +50% for roughness	0.01
Antenna supports	5 in. × $\frac{1}{2}$ in. D (two)	0.03	1.0	Figure 4.7	0.03
Interference					
Fuse vertical tail		0.11 (t^2)	0.05	Ref. 4.4	
Fuse horizontal tail		0.06 (t^2)	0.05		0.07
Fuse wing		0.6^2 (t^2)	0.1		
				Total	3.9 ft^2
Leakage?					
Cooling?					

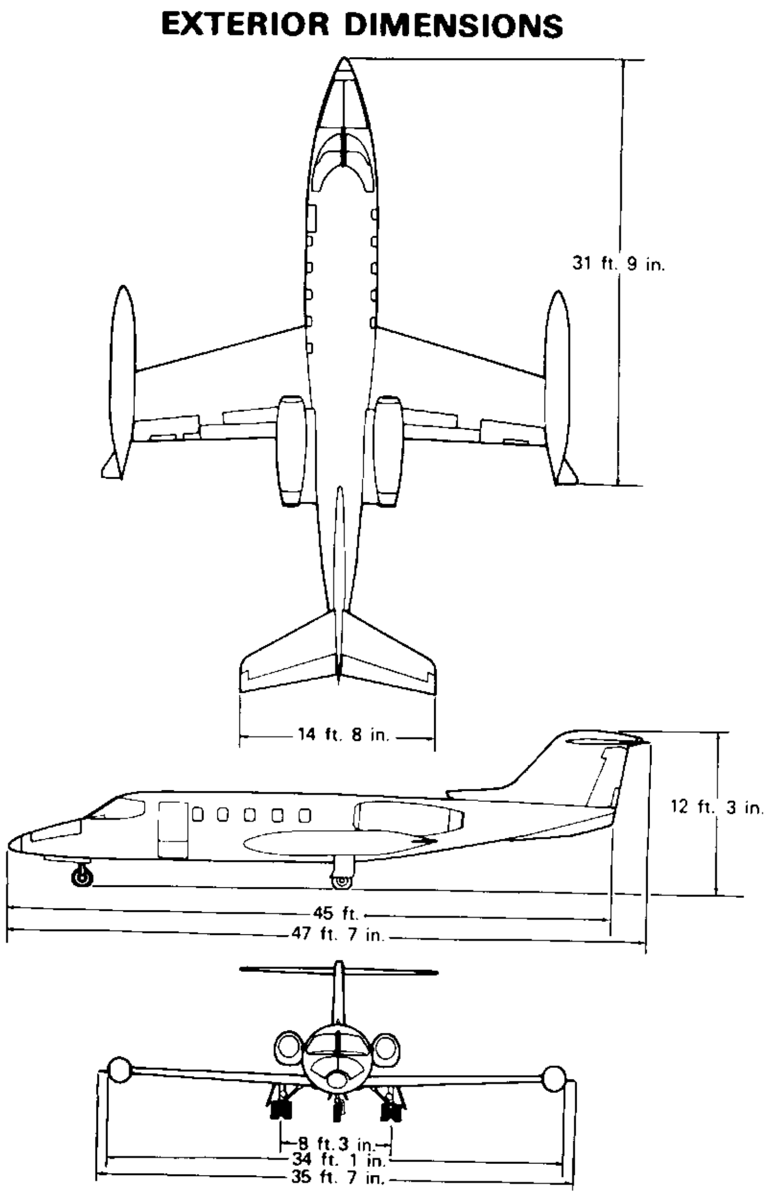

Figure 4.27 Gates Learjet Model 25. (Courtesy Gates Learjet Corp.)

Table 4.5 Parasite Drag Breakdown for Gates Learjet Model 25 (from Ref. 4.10)

Item	C_d (based on Wing Planform Area)	Percent of Total
Wing	0.0053	23.45
Fuselage	0.0063	27.88
Tip tanks	0.0021	9.29
Tip tank fins	0.0001	0.44
Nacelles	0.0012	5.31
Pylons	0.0003	1.33
Horizontal tail	0.0016	7.08
Vertical tail	0.0011	4.86
Interference	0.0031	13.72
Roughness and gap	0.0015	6.64
Total	0.0226	100.00

more like 0.4 or even higher instead of 0.04, as listed in Table 4.4. This would add another 0.06 m^2 (0.63 ft^2) to f.

Another example of a drag breakdown is provided by Reference 4.10. In this case, the airplane is the Gates Learjet Model 25 pictured in Figure 4.27. Table 4.5 was prepared on the basis of Reference 4.10. The authors of the reference chose to base C_d for each item on the wing area. This is therefore the case for Table 4.5, since dimensions and areas for each item were not available. Also, the reference did not include interference or roughness and gap drag in the parasite drag. Why this was done is not clear, and these two items are included in Table 4.5. These two somewhat elusive drag items are estimated to account for 20% of the parasite drag. Although not related to its parasite drag, according to Reference 4.10, this airplane has an Oswald's efficiency factor of 0.66.

TRIM DRAG

Basically, trim drag is not any different from the types of drag already discussed. It arises mainly as the result of having to produce a horizontal tail load in order to balance the airplane around its pitching axis. Thus, any drag increment that can be attributed to a finite lift on the horizontal tail contributes to the trim drag. Such increments mainly represent changes in the induced drag of the tail. To examine this further, we again write that the sum of the lifts developed by the wing and tail must equal the aircraft's weight.

$$L + L_T = W$$

Solving for the wing lift and dividing by qS leads to

$$C_{L_w} = C_L - C_{L_T}\frac{S_T}{S}$$

Here, C_{L_w} is the wing lift coefficient, C_L is the lift coefficient based on the weight and wing area, and C_{L_T} is the horizontal tail lift coefficient. The C_{D_i} of the wing, accounting for the tail lift, thus becomes

$$C_{D_{i_w}} = \frac{C_{L_W}^2}{\pi A e_w}$$

$$\simeq \frac{C_L^2}{\pi Ae} - 2\frac{C_L^2}{\pi Ae}\frac{C_{L_T}}{C_L}\frac{S_T}{S} \tag{4.38}$$

The term $[C_{L_T}(S_T/S)]^2$ has been dropped as being of higher order. Since $C_L^2/\pi Ae$ is the term normally defined as C_{D_i}, it follows from Equation 4.38 that the increment in the induced drag coefficient contributed by the wing because of trim is

$$\Delta C_{D_i} = -2C_{D_i}\frac{C_{L_T}}{C_L}\frac{S_T}{S} \tag{4.39}$$

The tail itself will have an induced drag given by

$$D_{i_T} = qS_T\frac{C_{L_T}^2}{\pi A_T e_T} \tag{4.40}$$

Expressed in terms of the wing area, this becomes

$$C_{D_{i_T}} = \frac{S_T}{S}\frac{C_L^2}{\pi Ae}\left(\frac{C_{L_T}}{C_L}\right)^2\frac{Ae}{A_T e_T} \tag{4.41}$$

Added to Equation 4.39 the total increment in the induced drag coefficient becomes

$$\Delta C_{D_{\text{trim}}} = \frac{S_T}{S}\frac{C_{L_T}}{C_L}\left(\frac{C_{L_T} Ae}{C_L A_T e_T} - 2\right)C_{D_i} \tag{4.42}$$

In order to gain further insight into the trim drag, consider the simplified configuration shown in Figure 4.28. For the airplane to be in equilibrium, it follows that

$$L_w + L_T = W$$
$$xL_w = (l - x)L_T$$

where l is the distance from the aerodynamic center of the wing to the aerodynamic center of the tail. x is the distance of the center of gravity aft of the wing's aerodynamic center. Solving for L_T gives

$$L_T = \frac{x}{l}W$$

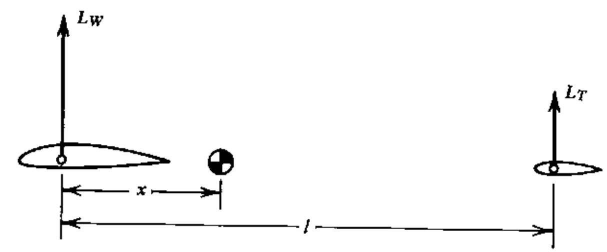

Figure 4.28 Equilibrium of wing and tail lifts.

Thus,

$$\frac{S_T C_{L_T}}{SC_L} = \frac{x}{l} \tag{4.43}$$

Substituting Equation 4.43 into Equation 4.42 leads to

$$\frac{\Delta C_{D_{\text{trim}}}}{C_{D_i}} = \frac{x}{l}\left[\frac{x}{l}\left(\frac{b}{b_T}\right)^2\frac{e}{e_T} - 2\right] \tag{4.44}$$

The ratio of the wingspan to tailspan is of the order of 3, while e is equal approximately to e_T. With these magnitudes in mind, Figure 4.29 was prepared; it presents the trim drag as a fraction of the original induced drag as influenced by x/l.

Notice that the possibility of a negative trim drag exists for small, positive, center-of-gravity positions. This results from the slight reduction in wing lift, and hence its induced drag, for aft center-of-gravity positions. However, as the center of gravity moves further aft, the induced drag from the tail overrides the saving from the wing so that the net trim drag becomes more positive.

The aerodynamic moment about the airplane's aerodynamic center was neglected in this analysis. By comparison to the moment contributed by the tail, M_{ac} should be small. Qualitatively, the results of Figure 4.29 should be relatively unaffected by the inclusion of M_{ac}.

The trim drag is usually small, amounting to only 1 or 2% of the total drag of an airplane for the cruise condition. Reference 4.10, for example, lists the trim drag for the Learjet Model 25 as being only 1.5% of the total drag for the cruise condition. As another example, consider the Cherokee once again at an indicated airspeed of 135 mph. At its gross weight of 2400 lb, this corresponds to a C_L of 0.322. For this weight the most forward center of gravity allowed by the flight manual is 3% of the chord ahead of the quarter-chord point. With a chord of 63 in. and the distance between the wing and tail aerodynamic center of approximately 13 ft, x/l has a value of -0.012. Since $b \simeq 3b_T$, Figure 4.29 gives

$$\frac{\Delta C_{D_{\text{trim}}}}{C_{D_i}} = 0.028$$

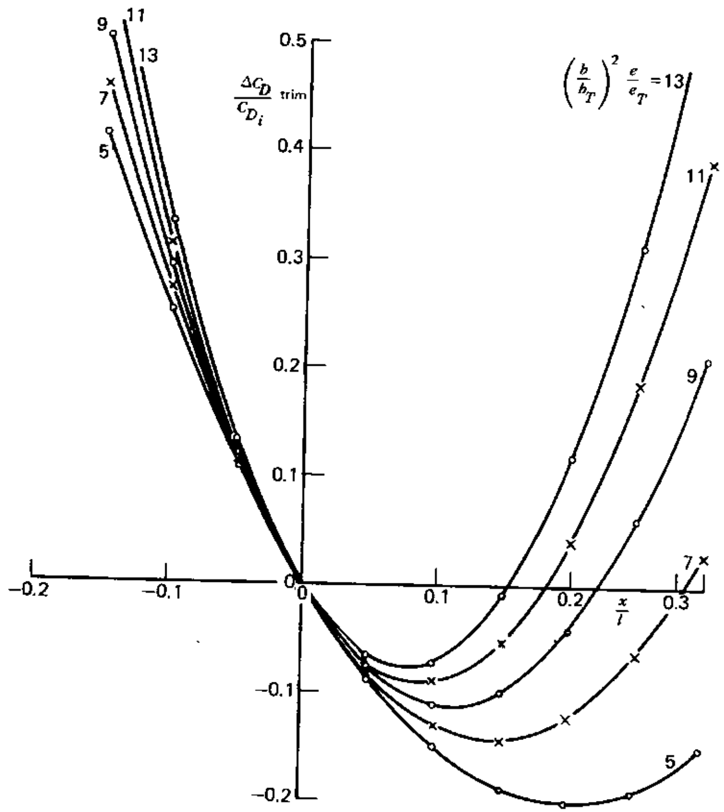

Figure 4.29 Effect of center-of-gravity position on trim drag.

With an effective aspect ratio of approximately 3.38, C_{D_i} will be equal to 0.0098, so that $C_{D_{trim}} = 0.0003$. The parasite drag coefficient is approximately 0.0037, so that the total C_D equals 0.0138. Thus, for the Cherokee in cruise, the trim drag amounts to only 2% of the total drag.

COOLING DRAG

Cylinder heads, oil coolers, and other heat exchangers require a flow of air through them for purposes of cooling. Usually, the source of this cooling air is the free stream, possibly augmented to some extent by a propeller slipstream or bleed air from the compressor section of a turbojet. As the air flows through the baffling, it experiences a loss in total pressure, Δp, thus extracting energy from the flow. At the same time, however, heat is added to

the flow. If the rate at which the heat is being added to the flow is less than the rate at which energy is being extracted from the flow, the energy and momentum flux in the exiting flow after it has expanded to the free-stream ambient pressure will be less than that of the entering flow. The result is a drag force known as cooling drag.

It is a matter of "bookkeeping" as to whether to penalize the airframe or the engine for this drag. Some manufacturers prefer to estimate the net power lost to the flow and subtract this from the engine power. Thus, no drag increment is added to the airplane. Typically, for a piston engine, the engine power is reduced by as much as approximately 6% in order to account for the cooling losses.

Because of the complexity of the internal flow through a typical engine installation, current methods for estimating cooling losses are semiempirical in nature, as exemplified by the Lycoming installation manual (Ref. 4.12). Before considering an example from that manual, let us examine the basic fundamentals of the problem. A cooler installation is schematically pictured in Figure 4.30. Far ahead of the cooling, free-stream conditions exist. Just ahead of the baffle, the flow is slowed so that the static pressure, P_B, and the temperature, T_B, are both higher than their free-stream values. As the flow passes through the baffle, P_B drops by an amount Δp because of the friction in the restricted passages. At the same time, heat is added at the rate Q, which increases T_B by the amount ΔT. The flow then exits with a velocity of V_E and a pressure of P_E, where P_E is determined by the flow external to the cowling. The exit area, A_E, and the pressure, p_E, can both be controlled by the use of cowl flaps, as pictured in Figure 4.31. As the cowl flaps are opened, the amount of cooling flow increases rapidly because of the decreased pressure and the increased area. Downstream of the exit, the flow continues to accelerate (or decelerate) until the free-stream static pressure is reached. Corresponding to this state, the cooling air attains an ultimate velocity denoted by V_∞.

If m represents the mass flow rate through the system, the cooling drag,

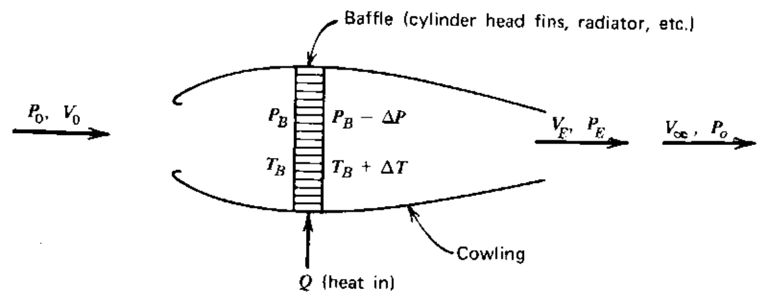

Figure 4.30 Schematic flow through a heat exchanger.

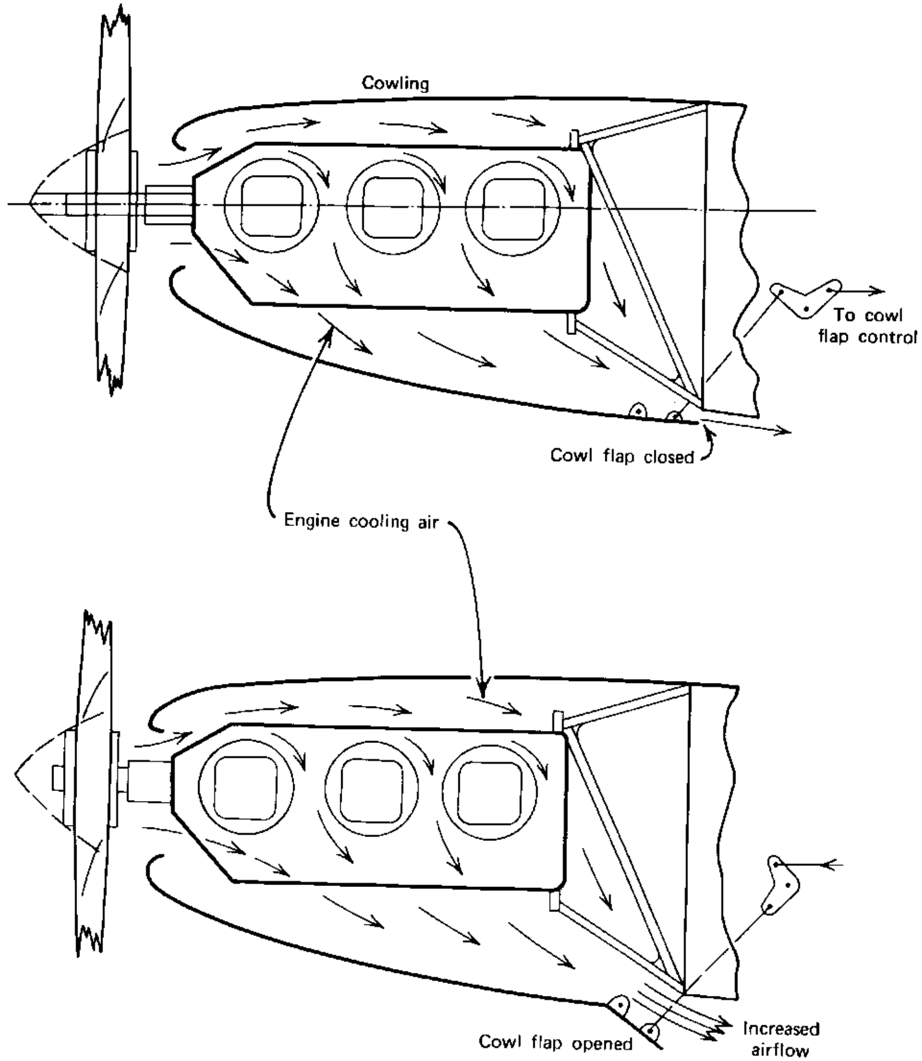

Figure 4.31 The use of cowl flaps to control engine cooling air. (*a*) Flow of cooling air around an air-cooled engine. (*b*) Typical cowl flaps on radial engine.

D_c, will be given by the momentum theorem as

$$D_c = m(V_0 - V_\infty) \tag{4.45}$$

The rate, ΔW, at which work is extracted from the flow is

$$\Delta W = \tfrac{1}{2}m(V_0^2 - V_\infty^2) \tag{4.46}$$

Observe that the cooling drag is obtained by dividing the increment in the

energy by a velocity that is the average between V_0 and V_∞; that is,

$$\Delta W = D_c\left(\frac{V_0 + V_\infty}{2}\right) \tag{4.47}$$

For a fixed-baffle geometry, the pressure drop through the baffle will be proportional to the dynamic pressure ahead of the baffle.

$$\Delta p \propto \tfrac{1}{2}\rho V_B^2 \tag{4.48}$$

V_B can be related to the mass flow, m, through the baffle and an average flow area through the baffle.

$$m = \rho A_B V_B \tag{4.49}$$

Substitution of Equation 4.49 into Equation 4.48 results in

$$\Delta p \propto \frac{m^2}{\rho} \tag{4.50}$$

In the preceding, for a fixed baffle, the fictitious area, A_B, has been absorbed into the constant of proportionality.

The rate at which heat is conducted away from the baffles by the cooling air must depend on the difference between the temperature of the baffles and that of the entering cooling air. For a piston engine, the baffle temperature is the cylinder head temperature (CHT). Denoting the cooling air temperature just ahead of the baffles by T_B, the rate of heat rejection by the engine can be written as

$$Q \propto \mathrm{CHT} - T_B \tag{4.51}$$

In Equations 4.50 and 4.51, the constants of proportionality will depend on the particular engine geometry and power. These constants or appropriate graphs must be obtained from the manufacturer. One is tempted to scale Q in direct proportion to the engine power, P, and to scale A_B with the two-thirds power of the engine power, in which case Equations 4.50 and 4.51 become

$$\Delta p \propto \frac{m^2}{\rho p^{4/3}} \tag{4.52}$$

$$Q \propto (\mathrm{CHT} - T_B)P \tag{4.53}$$

However, these are speculative relationships on my part; they are not substantiated by data and therefore should be used with caution.

If sufficient information is provided by the engine manufacturer to relate Δp, m, and ρ, and to estimate Q for a given temperature difference between CHT and the cooling air, then one is in a position to calculate the cooling drag. The details of this are best illustrated by means of an example given in Reference 4.12. In accordance with the reference, the English system of units will be used for this example.

This example will consider a horizontally opposed engine delivering 340 bhp operating at a 25,000 ft pressure altitude and a true airspeed of 275 mph. The outside air temperature is taken to be 20 °F higher than standard for this altitude, which means an OAT of −10 °F. Lycoming recommends 435 °F as a maximum continuous cylinder head temperature for maximum engine life. This example is to represent a cruise operation with cowl flaps closed. (This does not mean that the exit is closed; see Figure 4.31.) It is therefore assumed that the exit static pressure is equal to the ambient static pressure. Given the foregoing, the problem is to size the area of the exit and to calculate the cooling drag.

The mass density, ρ, can be calculated from the equation of state (Equation 2.1).

$$\rho = \rho_s \frac{T_s}{T}$$

where subscript s refers to standard values. From this, using Figure 2.3,

$$\rho = 0.00102 \text{ slugs/ft}^3$$

The free-stream dynamic pressure, q_0, is thus

$$q_0 = 83 \text{ psf}$$

Neglecting any contribution from the propeller slipstream for the cruise condition, the reference, on the basis of experience, calculates the temperature at the engine face by assuming a 75% recovery of the dynamic pressure with a resulting adiabatic temperature rise. From Equations 2.1 and 2.30,

$$\frac{T}{p^{[(\gamma-1)/\gamma]}} = \text{constant}$$

or

$$T_B = T_0\left(\frac{p_B}{p_0}\right)^{(\gamma-1)/\gamma}$$

$$= 450\left[\frac{786.3 + 0.75(83)}{786.3}\right]^{0.286}$$

$$= 460\ °\text{R}$$

Thus, the temperature at the engine face is 0 °F.

With the assumed 25% loss in dynamic pressure resulting from the diffusion by the cowling, the static pressure at the engine face, assuming the flow there to have a negligible velocity, will be

$$p_B = 848 \text{ psf}$$

This corresponds to a pressure altitude of 23,200 ft. Next, Figure 4.32 (provided by the manufacturer), is entered with the cooling air temperature at the engine face. For a CHT of 435 °F, this figure leads to a required cooling airflow of 2.55 lb/sec.

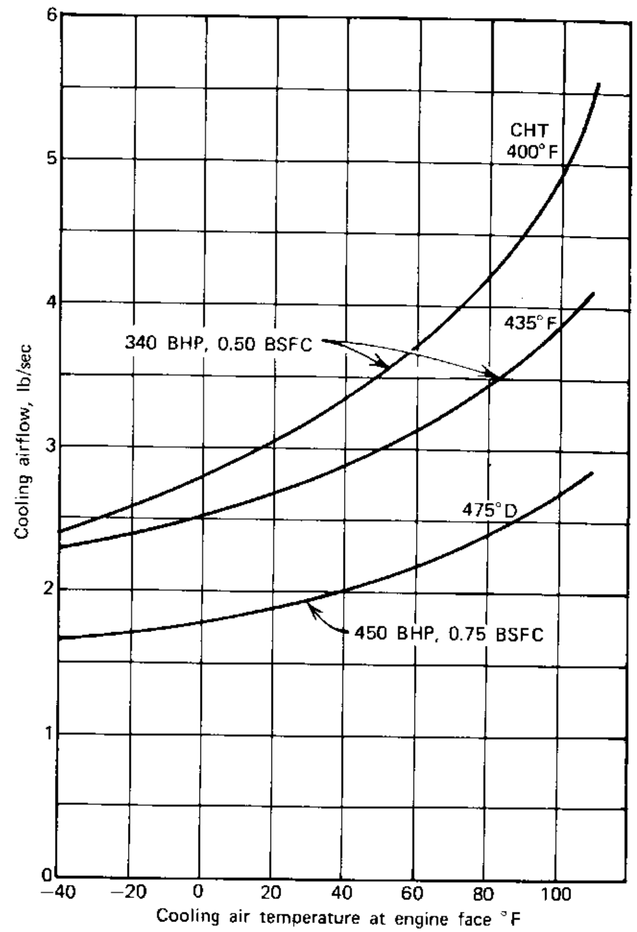

Figure 4.32 Required cooling airflow as a function of cooling air temperature at engine face.

The baffle pressure drop is determined next from Figure 4.33 (also provided by the manufacturer). It would seem, in accordance with Equation 4.50, that this graph should be in terms of the density altitude instead of the pressure altitude. Nevertheless, it is presented here as taken from Reference 4.12. Entering this graph with an airflow of 2.55 lb/sec at a pressure altitude of 23,200 ft results in a pressure drop of 47 psf. Thus, downstream of the cylinders, the total pressure will be

$$p_B - \Delta p = 801 \text{ psf}$$

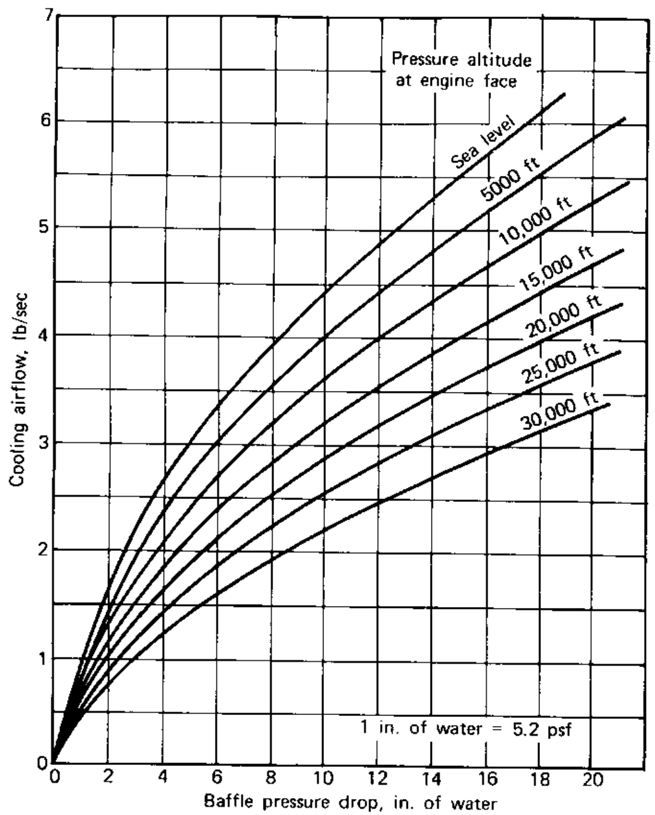

Figure 4.33 Baffle pressure drop as a function of cooling airflow.

Instead of using a heat flow, Q, per se, the reference assumes (presumably based on experience) that the cooling air will experience a temperature rise of approximately 150 °F across the cylinders. For this particular example, this temperature rise can be expressed in terms of Q by using the specific heat at constant pressure.

$$Q = C_p \Delta T m$$

For air $C_p \simeq 6000$ ft/lb/slug/°R. Thus, for the airflow of 2.55 lb/sec,

$$\begin{aligned} Q &= 6000(150)\frac{2.55}{32.2} \\ &= 71{,}273 \text{ ft-lb/sec} \\ &= 129.6 \text{ hp} \end{aligned}$$

Notice that the above rejected heat amounts to 38% of the engine power. This is close to the 40 to 50% quoted in other sources.

The cooling air density just downstream of the cylinder heads after the temperature rise can be calculated from the equation of state.

$$\begin{aligned} \rho_B' &= \frac{p_B - \Delta p}{RT} \\ &= \frac{801}{1711(460+150)} \\ &= 0.000767 \text{ slugs/ft}^3 \end{aligned}$$

This flow is then assumed to expand adiabatically to the ambient static pressure of 786 psf. Thus the density at the exit, from Equation 2.30, is found to be

$$\rho_E = 0.00076 \text{ slugs/ft}^3$$

The corresponding velocity is determined by the use of Equation 2.31.

$$\begin{aligned} V_E &= \left[\frac{2\gamma}{\gamma-1}\left(\frac{p_B - \Delta p}{\rho_B'} - \frac{p_E}{\rho_E}\right)\right]^{1/2} \\ &= \left[\frac{2(1.4)}{0.4}\left(\frac{801}{0.000767} - \frac{786}{0.000757}\right)\right]^{1/2} \\ &= 205 \text{ fps} \end{aligned}$$

This velocity, together with the density of the cooling flow at the exit and the required cooling flow, leads to a required exit area of 0.510 ft^2. This number, as well as V_E, differs slightly from Reference 4.12 as the result of calculating the flow state following the addition of heat in a manner somewhat different from the reference.

The resulting cooling drag for this example can be calculated from Equation 4.45.

$$\begin{aligned} D_c &= \frac{2.55}{32.2}(403 - 205) \\ &= 15.7 \text{ lb} \end{aligned}$$

This corresponds to an increment in the flat-plate area of 0.19 ft^2. In terms of engine bhp, assuming a propeller efficiency of 85%, this represents a loss of 10.2 bhp, or 3% of the engine power.

For operating conditions other than cruise, it may be necessary to open the cowl flaps. Reference 4.12 states that a pressure coefficient at the cowl exit as low as -0.5 can be produced by opening the flaps to an angle of approximately 15°. By so doing, a relatively higher cooling flow can be generated at a lower speed, such as during a climb. Even though the engine power may be higher during climb, operating with open cowl flaps and with a richer fuel mixture can hold the CHT down to an acceptable value. Also, CHT values higher than the maximum continuous rating are allowed by the manufacturer for a limited period of time.

It will not be repeated here, but Reference 4.12 also performs a calculation similar to the foregoing but for climb conditions at 19,000 ft pressure altitude, 450 bhp, mixture rich, 130 mph true airspeed, and an OAT of 31 °F. A CHT of 475 °F is allowed with the cowl flaps open to give an exit C_p of -0.5.

For this case, the required airflow is determined to be 1.95 lb/sec with an exit velocity of 73.8 fps. Thus, for this case,

$$D_c = 7.1 \text{ lb}$$
$$f_c = 0.32 \text{ ft}^2$$

The equivalent power loss is only approximately 0.5% of the engine power for this case, even though the increment in equivalent flat-plate area is appreciably higher than that in cruise.

DRAG REDUCTION

Skin friction drag and induced drag are the major contributors to the total drag of an airplane, at least for a modern jet transport. For lower-speed, general aviation aircraft, form drag assumes more relative importance. A typical drag buildup (or breakdown, depending on your outlook) is presented in the bar graph of Figure 4.34 for a jet transport, as reproduced from

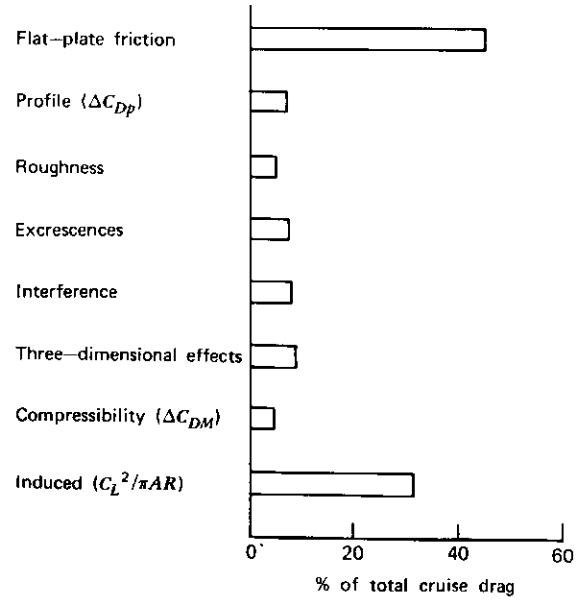

Figure 4.34 Typical drag buildup for jet transport.

Reference 4.11. It is seen that skin friction drag and induced drag account for approximately 75% of the total drag. Although the remaining 25% is not to be taken lightly, the potential for real savings in power or fuel rests with reducing the skin friction drag and induced drag.

Winglets

A recent development that holds some promise for reducing induced drag, short of increasing the aspect ratio, is the so-called winglet. The details of a winglet (studied in Ref. 4.15) are shown in Figure 4.35; Figure 4.36 pictures the winglet mounted on the wing tip of a first-generation jet transport (such as a Boeing 707).

The winglet is reminiscent of the tip plate, which has been tried over the years for the same purpose. These plates have never proven very successful for reasons that will become clear as the details of the winglet design are discussed.

Placing the winglet on an existing wing will alter the spanwise distribution of circulation along the wingspan and hence the structure of its trailing vortex system far downstream. One can calculate the reduction in the induced drag afforded by the winglet solely by reference to the ultimate wake, or so-called Treffetz plane. This is the method used by Reference 4.17 together with a numerical vortex-lattice, lifting-surface theory. Examining only the ultimate wake is not very satisfying, however, from a physical standpoint. Instead, consider the flow field into which the winglet is inserted.

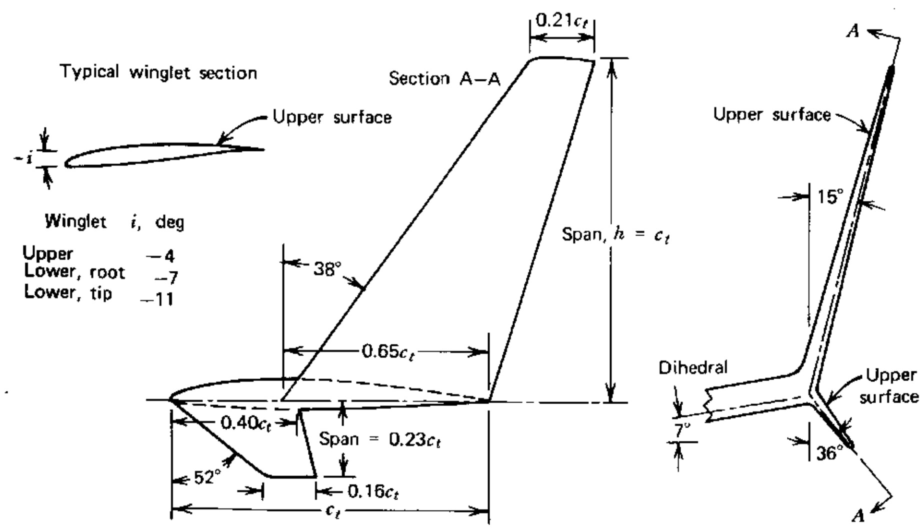

Figure 4.35 Winglet geometry.